communications earth & environment

Article

A Nature Portfolio journal

https://doi.org/10.1038/s43247-025-02576-8

Biogeochemical impact of nickel and urea in the great oxidation event

Dilan M. Ratnayake [1,2] ✉, Ryoji Tanaka [1] ✉ & Eizo Nakamura[1]

The Great Oxidation Event marks the first substantial increase in atmospheric oxygen on Earth. Despite the oxygenic photosynthesis that emerged hundreds of million years before this event, the specific biogeochemical mechanisms responsible for maintaining low oxygen levels for an extended period remain elusive. Here, we show the critical role of urea as a nitrogen source for cyanobacteria, the cascading impact of nickel on abiotic urea production, and their combined effects on the proliferation of cyanobacteria leading to the great oxidation event. Urea formation was experimentally evaluated under simulated Archean conditions and cyanobacterial growth was monitored providing urea as the nitrogen source. Our findings demonstrate that urea can be produced in the Archean cyanobacterial habitats with UV-C irradiation, shedding light on the controversy regarding the evolution of nitrogen-fixing enzymes in primitive cyanobacteria. We propose that environmental conditions in the early Archean, characterized by elevated urea and nickel concentration, may have hindered cyanobacterial expansion, contributing to the delay between the evolution of oxygenic photosynthesis and the onset of the great oxidation event.

The origin and evolution of cyanobacteria are intricately associated with atmospheric evolution because they are the sole known oxygen-producing organisms to have existed on early Earth. Understanding the biogeochemical parameters that influenced the growth of these microorganisms is crucial for a better understanding of the cause and dynamics of the Great Oxidation Event (GOE), which occurred 2.4–2.1 billion years ago (Ga)[1]. Nutrient availability, particularly nitrogen, plays an important role in microbial ecosystems, affecting their growth and, therefore, the net oxygen production in cyanobacteria[2,3]. Although geochemical evidence indicates an early evolution (~3.2 Ga) of nitrogen fixation (conversion of atmospheric N_2 into NH_3) via the nitrogenase enzyme[4,5], phylogenetic data suggest its development in cyanobacteria after the GOE[6,7]. Preventing the deactivation of nitrogenase by oxygen[8–10] may have posed a major challenge for primitive cyanobacteria, given the ongoing debates on the timing of the evolution of nitrogenase protective strategies such as developing heterocyst[11–16]. Besides protecting nitrogenase, the heterocysts also improvise the cells to function under low concentrations of Mo[3], which is essential for the functioning of nitrogenase. However, the scarcity of Mo in anoxic environments[8,17] raises questions regarding the evolutionary early use of the Mo isoform of nitrogenase, supported by culture experiments demonstrating reduced growth rates in nitrogen-fixing cyanobacteria under low Mo levels[3,18]. Nevertheless, the phylogenetic studies and geochemical evidence indicate that the evolution of the Mo isoform of nitrogenase preceded its V- and Fe-dependent isoforms[4,6,19].

Alternatively, abiotic conversion of atmospheric N_2 into fixed nitrogen forms like ammonium (NH_4^+), hydrogen cyanide (HCN), or NO_x species could have provided bioavailable nitrogen during the Archean. The deficit of abiotically produced NO is postulated as a driver for the evolution of biological nitrogen fixation[20] or it is assumed that biological nitrogen fixation evolved as a protective mechanism against cyanide-induced damage[21]. Considering the potential high abundance of urea (H_2NCONH_2) in ancient Earth[22] and the documented constitutive urease activity in phylogenetically distant cyanobacteria[23], urea also emerges as a plausible nitrogen source for primitive organisms. If urea indeed served as a nitrogen source, the availability of Ni may have played a critical role because of its requirement for the functioning of urease enzyme[24,25] which is responsible for converting intracellular urea into biologically useful NH_4+. Therefore, given the documented decline in Ni flux to the Precambrian Ocean[26], an evaluation is warranted regarding the combined effects of Ni and urea on cyanobacterial growth.

This work comprises two interconnected components. First, we investigated the capability of forming urea from dilute cyanide (CN^-) solutions under UV-C irradiation, simulating conditions common in the Archean. Secondly, we conducted growth experiments on unicellular cyanobacteria (*Synechococcus sp.* PCC 7002) to investigate the influence of urea

[1]The Pheasant Memorial Laboratory for Geochemistry and Cosmochemistry, Institute for Planetary Materials, Okayama University, Misasa, Tottori, 682-0193, Japan. [2]Present address: Department of Geology, University of Peradeniya, Peradeniya, 20400, Sri Lanka. ✉e-mail: dilanrath@s.okayama-u.ac.jp; ryoji@okayama-u.ac.jp

and Ni for their growth. Combining the experimental results with current knowledge on Archean bio-geo dynamics, we aim to establish a theoretical framework that explains the temporal gap between the onset of oxygenic photosynthesis and the GOE.

Results and Discussion

Urea formation by UV-C irradiation

The UV-C irradiation (200–280 nm), which was more intense before the development of the ozone layer (ca. 2.4 Ga)[27], is proposed as an inhibitor of the limited expansion of cyanobacteria[28]. Despite the stressful effects of UV-C irradiation on primitive life forms, chemical compounds could have utilized this valuable photon energy to yield vital compounds. Experimental studies demonstrated that exposing concentrated ammonium cyanide solutions to UV-C irradiation results in urea formation[29], although the prevalence of such concentrated solutions in Archean cyanobacterial habitats is questionable. Thus, the production of urea via UV-C irradiation was examined with continuous UV-C irradiation (≥7 days, 254 nm) on dilute mixtures of ammonium chloride [NH_4Cl], ferrocyanide [$K_4Fe(CN)_6$], and sodium cyanide [NaCN] (Supplementary Table 1). Urea was formed across all the irradiated solutions, implying its readily formation in potential Archean environments (Fig. 1). The production of urea correlated positively with the amounts of ferrocyanides and NH_4^+ (Fig. 1a, c), likely due to increased production and stabilization of OCN^- in the medium, allowing its reaction with NH_4^+ to form urea: $OCN^- + NH_4^+ \rightarrow H_2NCONH_2$. While CN^- is essential for forming ferrocyanides, the availability of free CN^- showed an inverse correlation with urea yields (Fig. 1d), indicating minimal direct photooxidation of CN^- to OCN^-[30]. Furthermore, the stability of ferrocyanide in slightly alkaline solutions[31] contributed to higher urea yields compared to slightly acidic mixtures (Supplementary Table 1, Supplementary Fig. 1). Widespread methanogenesis likely provided sufficient CH_4[32,33], enabling the photochemical production of HCN[34,35], a major source of CN^- during the Archean, in addition to other minor contributions[36,37]. Instantaneous ferrocyanide formation[31] and availability of NH_4^+[35,36,38–46], together with the observed urea production in experiments, might have led to rapid accumulation of urea in the Archean cyanobacterial habitats due to its stability against UV and γ irradiation[47,48]. Based on the steady-state HCN concentrations in primitive oceans[49] and the urea yields obtained from this study, urea could have been accumulated within a short period under wide range of potential Archean conditions (with an oceanic pH ranging from 6.4 to 7.4 and temperature of 23 °C–75 °C under HCN deposition rates of 50–500 nmol cm^{-2} yr^{-1} see Supplementary Table 2, 3 and Supplementary Fig. 2). The hydrothermal recharge zones could act as decomposition sites for the produced urea[50]. However, the modern ocean circulates only 0.02% of water mass as hydrothermal flux[51] and the average time for the whole ocean to circulate through hydrothermal systems is estimated as 8–10 million years[52]. Therefore, urea decomposition in these settings is negligible even with a several-fold increased hydrothermal activity during the Archean. Moreover, even if urea is degraded, the resulting NH_4^+ may enhance the urea production as envisaged in the experiments (Fig. 1a).

Cyanobacterial Culture Experiments

Cyanobacterial growth experiments were conducted to explore the role of urea as a nitrogen source (see Methods). Figure 2a, b show the growth curves of cyanobacterial cultures in a modified A+ medium (Supplementary Table 4), with varying urea and Ni concentrations (U_xN_y, x mmol L^{-1} of urea and y nmol L^{-1} Ni). Growth was monitored for 15–18 days and optical density (OD) at 750 nm (OD_{750}) was recorded daily to monitor cell growth. Broken lines in the growth curves in Fig. 2b represent the cultures that lost their pigmentation (hereafter referred to as bleached, Fig. 2d) at the stationary phase of the growth and solid lines represent healthy growth. Results indicate that the ability of urea to serve as a nitrogen source for cyanobacteria depends on its concentration. At urea concentrations ≥2 mmol L^{-1},

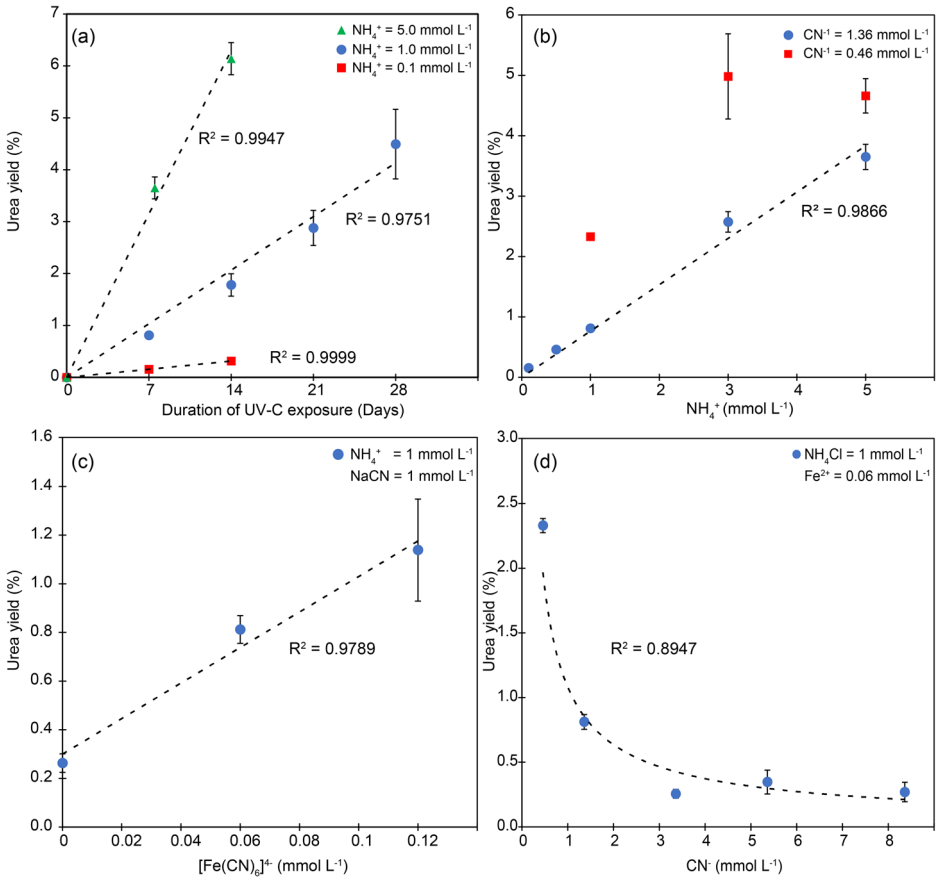

Fig. 1 | Urea yields in different experimental conditions. a Influence of duration of UV-C irradiation, **b** availability of NH_4^+, **c** Fe^{2+}, **d** CN^- on urea yield. Trendlines were calculated based on linear (**a**,**b**,**c**) and power (**d**) regression and error bars plotted as 2 SD.

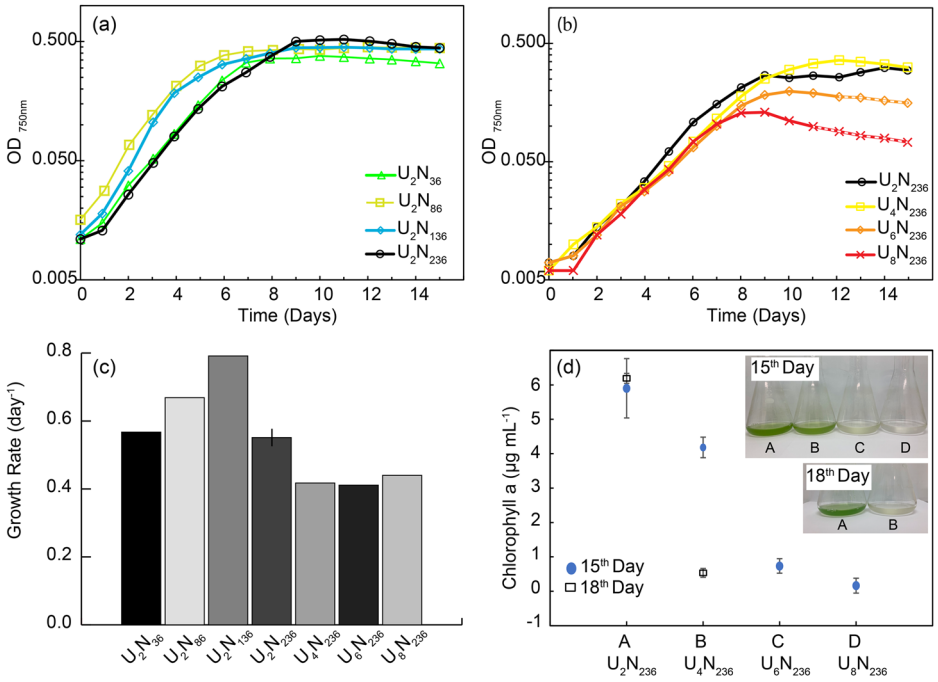

Fig. 2 | Growth information for PCC 7002. Varying (**a**) Ni and (**b**) urea concentrations. Unfilled lines represent bleached cultures. **c** Growth rates of bacterial cultures. **d** Chlorophyll_a concentration (normalized to the OD_{750}) measured on the 15th and 18th days of growth.

the cyanobacteria bleached during their stationary growth phase (Fig. 2d), possibly due to excessive intracellular NH_3 accumulation[53,54]. However, the inverse relationship between urea concentration and the time to initiate cell bleaching (indicated by low chlorophyll-a concentration, Fig. 2d) suggests a maximum tolerable level of urea around 2 mmol L^{-1} for cyanobacteria. Therefore, growth experiments suggested that the growth of primitive cyanobacteria could have been restricted beyond this urea concentration. On the other hand, the high urea tolerance observed in the most ancient methanogens[55,56] indicates that methanogenesis could have been sustained despite the prevalence of high urea concentration in the growth medium.

Further growth experiments varying Ni concentration of the growth medium at constant urea concentration of 2 mmol L^{-1} revealed the fastest growth rates (day^{-1}) in U_2N_{136} cultures (0.79), followed by U_2N_{86} (0.67), U_2N_{36} (0.60), and U_2N_{236} (0.57), indicating an optimal Ni concentration of 136 nmol L^{-1} (Fig. 2a, b) and growth inhibition beyond it. Fast growth rates with increasing Ni concentrations may have resulted from enhanced urease activity due to the presence of Ni[57] but oxidative stress caused by excessive Ni[58] could have slowed the growth beyond a Ni concentration of ~136 nmol L^{-1}. Previous study[57] has reported an optimal Ni concentration of 5 μmol L^{-1} for the growth of PCC 7002 in a urea-supplemented medium. The discrepancy may be attributed to the use of EDTA in the previous study[57], as EDTA can form a Ni-EDTA complex in the medium, reducing the availability of free Ni ions. Consequently, our finding suggests that the optimal Ni concentration required for cyanobacteria to utilize urea is about two orders of magnitude lower than previously recognized. Thus, the proposed evolution of seawater Ni concentrations, which were mostly >150 nmolL^{-1} until the Neoarchean[26,59] could have limited the cyanobacterial growth together with high urea concentrations as envisaged by our experiments.

In addition to Ni, several other metals can also affect cyanobacterial growth especially when they utilize urea as a nitrogen source. Studies on urease inhibition conducted in vitro reveal that the inhibition constant increases, meaning the inhibitory effect decreases in the following order: Hg^{2+}, Cu^{2+}, Zn^{2+}, Cd^{2+}, Ni^{2+}, Pb^{2+}, Co^{2+}, Fe^{3+} and As^{3+}[60]. Despite the presence of high concentrations of Cu and Zn in the A+ growth medium without EDTA (Supplementary Table 4), the observed cellular growth indicates that either the cyanobacterial cells can overcome these inhibitory effects in vivo, or the effects are negligible. Furthermore, most of these urease-inhibiting metals could have been removed as sulfides or precipitated with Fe(II) silicate minerals under sulfidic or ferruginous conditions, respectively, during the Archean era[61].

In contrast to the growth inhibitory effects observed in liquid media, the prolonged growth observed on agar plates yielded valuable insights into the adaptability of cyanobacteria attached to surfaces like microbial mats. Unlike in liquid media, bacterial growth occurred across all tested Ni concentrations (10–1000 nmol L^{-1}) on agar plates with urea levels exceeding 2 mmol L^{-1} (i.e., 10 mmol L^{-1}). Cell bleaching on agar plates only occurred when urea concentration >>10 mmol L^{-1} (i.e., 50 mmol L^{-1}), regardless of Ni concentration. The slower nutrient diffusion in agar may reduce growth inhibitory effects, explaining differences in cell growth between liquid and agar media. These findings suggest that a reduction of the bioavailability of urea and Ni could mitigate their growth inhibitory effects.

What caused the delay in atmospheric oxygenation?

This study suggests that the high Ni and urea availability in the early Archean could have stifled cyanobacterial growth, while favoring methanogenesis, thus sustaining a methane-rich atmosphere[32,33] conducive to HCN and urea production (Fig. 3). Evidence for methanogenesis dates back >3.46 Ga[33] or even 4.1 Ga[62] and evidence for free oxygen supports the presence of cyanobacteria from 2.9 Ga[63]. If so, urea could have formed and accumulated for ~0.6–1.2 billion years from the origin of methanogenesis. Our calculations suggest that this time is enough to accumulate high urea levels (≥2 mmol L^{-1}) (Supplementary Table 2,3). Eventually, the reduced influx of Ni into the ocean, at the onset of Neoarchean era[26,59], may have lowered the deposition rates of HCN, ultimately leading to a decrease in urea production.

The gradual decrease in urea and Ni concentrations may have initially facilitated long-term growth of ancient benthic cyanobacterial species[64]. These organisms could have adhered to surfaces that were occasionally inundated in shallow marine environments, influenced by temporal and spatial changes in urea bioavailability. This phenomenon could have occurred even under high urea levels as demonstrated by our bacterial growth experiments on agar plates. This supports the idea that ancestral cyanobacteria primarily lived as an attached organism rather than a free-floating species[13].

In fact, there is evidence of ancient benthic cyanobacterial species which form microbial mats (e.g., ref. 65.) which could have contributed

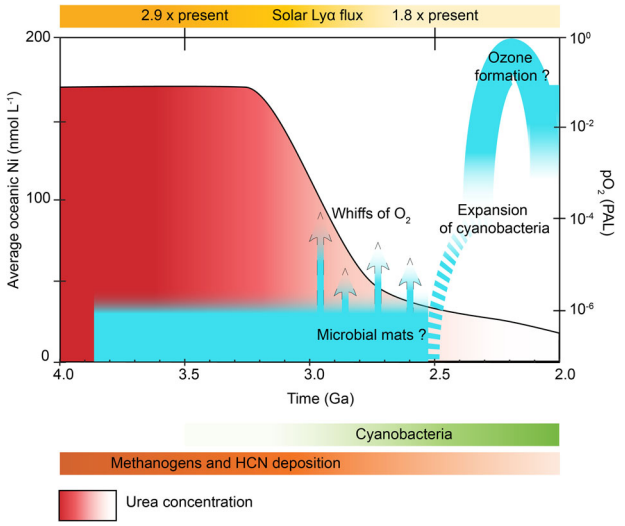

Fig. 3 | Graphical representation of the events lead to GOE. The solid curve represents the average dissolved oceanic Ni concentration (nmol L^{-1}). Light blue indicates pO_2 (Present Atmospheric Level, PAL). Changes in urea concentration are indicated by a red gradient (darker red represents higher concentrations). The average dissolved oceanic Ni concentration is plotted on data from ref. 26, and the Oxygen evolution curve is from ref. 1. Solar Lyman α flux is from ref. 83.

small but considerable amounts of oxygen globally before the GOE, at a time when urea levels were still high enough to inhibit unattached (planktonic) growth. As urea concentrations continued to decline (for example, to 4 mmol L^{-1}), it may have allowed for the occasional short-lived free-floating cyanobacterial blooms (Fig. 2d), which would have also increased the organic burial.

Collectively, these scenarios can explain evidence for transient and localized oxygenated conditions[66–68] that preceded the GOE (i.e., 3–2.5 billion years ago). Extended periods of cyanobacterial growth, accompanied by larger biomass likely became more feasible as urea concentrations decreased < ~4 mmol L^{-1}, eventually contributing to increased oxygen production and onset of the GOE (Fig. 3).

After the onset of the GOE, gradual increase in oxygen levels could have facilitated the oxidation of NH_4^+, further limiting urea production. In addition, the formation of the ozone layer due to the atmospheric O_2 accumulation could have reduced UV-C irradiation reaching the Earth's surface, inhibiting the photochemical reactions necessary for urea production. While the supply of urea was reduced by these processes, the rate of urea consumption by the larger cyanobacterial biomass increased, ultimately limiting the bioavailable nitrogen. This could have created evolutionary pressure for alternative nitrogen sources, possibly driving the evolution of nitrogen fixation through nitrogenase or the adaptation of existing nitrogenase/detoxyase in cyanobacteria[20,21]. If nitrogenase had already evolved in cyanobacteria, its activity might have been suppressed due to the preferential uptake of urea (see[2] and references therein). Once the urea source was depleted its activity could have resumed: however, it may have been compromised by oxygen in the absence of protective mechanisms. This situation could have resulted prolonged oxygen stasis throughout the majority of the Proterozoic[11].

On the other hand, if cyanobacteria were capable of fixing nitrogen before the GOE, explaining the increase of oxygen to modern levels during the Lomagundi excursions and its subsequent decline[69,70] becomes challenging. This is particularly true unless large differences existed in the bioavailability of other nutrients such as phosphorus.

In addition to nitrogen, phosphorous can limit the primary productivity[71] and therefore considered a crucial factor in ocean-atmospheric oxygenation[72,73]. Although there are theories suggesting that phosphorus delivery occurred due to the emergence of continents in the early or late Archean[74–76] and that phosphate recycling was aided by UV degradation of organic phosphorus compounds[77], the pervasive Fe-rich conditions may restrict phosphorus bioavailability[73]. However, the experimental studies on filamentous cyanobacterial species have demonstrated that availability of reduced nitrogen enhance the growth rates and photosynthetic activity irrespective of phosphorus availability and reduced the N_2 fixation rates[2]. The same study reveals that phosphorus limitation does not affect nitrogen fixation rates may be due to various adaptations displayed by cyanobacteria to cope with phosphorus limitation[78,79].

Though we propose the potential use of urea as the nitrogen source throughout the Archean, existing trends in nitrogen isotope records have been interpreted as originating from Mo nitrogenase, thus supporting an early evolution of nitrogen fixation[4]. It is important to note that nitrogen isotope fractionation upon urea assimilation falls within the range produced by Mo-nitrogenases[80–82]. However, the extent of fractionation during N_2 and $K_4Fe(CN)_6$ photodissociation by EUV/UV photons in the Archean Earth[83] would have defined the isotope composition of urea and, therefore, the ultimate nitrogen isotope signature. Previous studies have rejected atmospheric sources of nitrogen based on the idea that photodissociation reactions would largely fractionate organic nitrogen compounds. However, organic aerosol formation from UV irradiation of CH_4-N_2 gas mixtures[84,85] revealed that the nitrogen isotope composition of the aerosols depends on the CH_4 concentration. Based on these results, it can be expected that HCN, the source of CN^-, would acquire a similar isotopic composition to atmospheric N_2 due to the proposed high CH_4 levels (>5000 ppmv[32]) in the Archean. Isotope fractionation during the subsequent reactions (see Supplementary Discussion) requires evaluation in future studies, but our model provides a new framework for interpreting observed N isotope signatures in ancient geological samples.

Conclusions

We propose that Ni availability, methanogenesis, and urea production were intimately connected, with high urea (>2 mmol L^{-1}) and Ni (>136 nmol L^{-1}) levels inhibiting the growth and expansion of cyanobacteria in early Archean. Growth-favorable conditions occurred as Ni and urea concentrations decreased, first, allowing intermittent short-lived cyanobacterial blooms and later, extended growth periods of large biomass, contributing to the eventual rise in atmospheric oxygen, namely the GOE. If this hypothesis is correct, Ni plays a key role in understanding the complicated history of the GOE and the associated geochemical signatures.

Methods

Reagents and materials

Water used in the experiments was prepared using a Milli-Q system (Merck Millipore, France) and had a conductivity of >18.2 MΩ cm^{-1}. Electronic (EL) grade 36% HCl (Kanto Chemical), and EL grade 70% HNO_3 (Kanto Chemical) were distilled by a PFA sub-boiling distillation apparatus. The distilled reagents are referred with a 1D (distilled once) or 2D (distilled twice) prefix before the acid name. The recipe of the culture medium is shown in Supplementary Table 4. Glassware used for cell growth was pre-cleaned by soaking in 5 mol L^{-1} HCl (Special Grade, Fujifilm Wako Pure Chemical), a diluted, high-purity alkaline detergent (TMSC, Tama Chemicals), and 4 mol L^{-1} HCl (EL) for >12 h each. After each soaking step, the glassware was rinsed five times with water and stored. Quartz screw vials (99.99% quartz, 10 ml, Fujifilm Wako Pure Chemical) used for UV-C irradiation experiments were cleaned similarly to the method used to clean glassware used for cell growth. Special grade reagents of NH_4Cl (99.5%, Fujifilm Wako Pure Chemical), $K_4Fe(CN)_6$ (99.5%, Fujifilm Wako Pure Chemical) and NaCN (>97%, Special grade, Kanto Chemical) were dissolved in water to make stock solutions of desired concentration one day before the initiation of each experiment. The UV irradiation experiments were conducted using UV lamp (SLUV-4, AS ONE) with the wavelength set to 254 nm.

Cell growth conditions

Synechococcus sp. PCC 7002 was purchased from the Laboratoire Collection des Cyanobactéries, Institut Pasteur, France. The cells were grown

photoautotrophically either in agar or liquid medium with modified A+ composition[86] without EDTA and NO_3^- (Supplementary Table 4). The EDTA was omitted to more accurately assess the growth-limiting metal concentrations. Urea and trace metals were added to the autoclaved growth media using syringe filters (0.2 μm, Advantec, Japan). No CO_2 bubbling was carried out in any of the experiments.

The PCC 7002 was cultured in the media with varying concentrations of urea and Ni, and each medium was expressed as UxNy (x mmol L^{-1} of urea and y nmol L^{-1} of Ni) as listed in Supplementary Table 5. The maximum Ni concentration was chosen based on the average dissolved Ni in Precambrian Ocean[26], and the upper limit for urea was based on previous bacterial culture experiments[54]. Bacteria grown on U_2N_{36} were inoculated into liquid medium (1% V/V), and the cultures were then maintained under a 12 h light and 12 h dark cycle with a light intensity of 200 μmol m^{-2} s^{-1} in a thermostatic water bath (Thomas Kagaku Co., Japan). The culture media were shaken at 60 rpm, and the temperature was kept at 38 ± 0.1 °C throughout the experiment. The photoperiod, light intensity, and temperature for the agar media were also similar to those for the liquid media. The use of 750 nm wavelength for OD measurements is less susceptible to interference from pigments and corresponds to particle density[87]. Therefore, OD_{750} was used as a proxy for cell number. The OD_{750} measurements were taken daily using a spectrophotometer (ASV11DH, AS ONE, Japan) for ~15 days (Supplementary Table 6) and the growth rate (μ) was calculated using the exponential portion (U_2N_y – 1st to 4th day, U_xN_{236} – 2nd to 5th day) of the growth curves by the use of the equation: ($\mu = \ln(OD_2/OD_1)/(t_2 - t_1)$). Chlorophyll_a was extracted using methanol as a solvent[88] and the concentration was calculated using the equation: chlorophyll a (μg mL^{-1}) = 12.9447 × ($A_{665} - A_{720}$) (A_i = absorbance at i wavelength)[89] (Supplementary Table 7). The Ni blank in agar medium and liquid medium were measured by a sector field type ICP-MS (ELEMENT XR, Thermo Scientific, Germany) using an isotope dilution technique[90].

UV-C irradiation experiment

Mixtures of NH_4Cl, NaCN and $K_4Fe(CN)_6$ (Supplementary Table 1) with varying concentrations were prepared in quartz vials. The concentrations of NH_4^+ and Fe used were based on the proposed concentrations in the Precambrian Ocean[32]. The pH was adjusted to the desired values using NaOH and HCl before the initiation of the experiment. The vials were tightly sealed and placed in a custom-built UV irradiation chamber at room temperature (23 ± 1 °C). They were then exposed to 254 nm UV irradiation (0.614 mW cm^{-2}) for the specified duration. This irradiance is comparable to that predicted for the Archean (0.4 mW cm^{-2})[27]. Samples were taken weekly during each experimental session, and urea concentrations were determined by the colorimetric method using diacetyl monoxime with strong acids as described elsewhere[91]. Urea yield is expressed relative to the initial CN^- concentration. Each experiment was carried out in triplicate.

Urea accumulation time

Urea yields were calculated based on the steady-state HCN concentration obtained using Eqs. M1–M4 (See ref. 49 for more information on the calculation of steady-state HCN concentrations) of the ocean, assuming it has a volume of 300 L cm^{-2} and covers the whole Earth with a surface area of 5.10×10^{18} cm^2 and pH was fixed either to 6.4, 7.4 or 8.4. The percentages of CN^- converted into urea were chosen to represent the highest and lowest urea production yield (after a 7-day exposure period) based on experiments. To compensate for daylight duration of 12 h the maximum and minimum percentages of CN^- converted into urea in a week were divided by two. The maximum percentage of 2.5% is based on experiment F (Supplementary Table 1) and the minimum percentage of 0.05% was chosen arbitrarily to represent the lowest percentage of CN^- converted into urea in a week. Note that this minimum percentage is lower than the lowest obtained in the experimental conditions (see Supplementary Table 1). It was also assumed that urea production correlated linearly with ocean depth, did not vary with the temperature and that any sinks for urea were negligible. To calculate the time needed to accumulate 2 mmol L^{-1} of urea, scenarios in which homogenous production occurs in the ocean and production confined up to a depth of 30 m (0.81 % of the average oceanic depth) considered and results are shown in Supplementary Table 2 and 3, respectively.

$$pK_w = -0.60846 + \frac{4471.33}{T} + 0.017053T \quad \text{(M1)}$$

$$pK_{HCN} = -8.85 + \frac{3802}{T} + 0.01786T \quad \text{(M2)}$$

$$\log k_2^{OH-} = 16.62 - \frac{4440}{T} \quad \text{(M3)}$$

$$\sum HCN = \frac{S}{V_0} \times \frac{[(H^+) + K_{HCN}]}{k_2^{OH-} \times K_w} = \frac{S}{V_0 k_1} \quad \text{(M4)}$$

K_w = Ionic product of water
k_2^{OH-} = Rate constant of the base catalyzed hydrolysis
K_{HCN} = Equilibrium constant of HCN
S = HCN production rate in (nmol cm^{-2} yr^{-1})
V_0 = Volume of Ocean (L cm^{-2})
T = Temperature (K)
ΣHCN = HCN + CN^- = steady state HCN concentration

Data availability

Data for this manuscript are available at the Figshare repository with the following link, https://doi.org/10.6084/m9.figshare.29511983.

Received: 5 November 2024; Accepted: 11 July 2025;
Published online: 12 August 2025

References

1. Lyons, T. W., Reinhard, C. T. & Planavsky, N. J. The rise of oxygen in Earth's early ocean and atmosphere. *Nature* **506**, 307–315 (2014).
2. Kramer, B. J., Jankowiak, J. G., Nanjappa, D., Harke, M. J. & Gobler, C. J. Nitrogen and phosphorus significantly alter growth, nitrogen fixation, anatoxin-a content, and the transcriptome of the bloom-forming cyanobacterium, Dolichospermum. *Front. Microbiol.* **13**, 1–22 (2022).
3. Glass, J. B., Wolfe-Simon, F., Else, J. J. & Anbar, A. D. Molybdenum-nitrogen co-limitation in freshwater and coastal heterocystous cyanobacteria. *Limnol. Oceanogr.* **55**, 667–676 (2010).
4. Stüeken, E. E., Buick, R., Guy, B. M. & Koehler, M. C. Isotopic evidence for biological nitrogen fixation by molybdenum-nitrogenase from 3.2. *Gyr. Nat.* **520**, 666–669 (2015).
5. Beaumont, V. & Robert, F. Nitrogen isotope ratios of kerogens in Precambrian cherts: A record of the evolution of atmosphere chemistry? *Precambrian Res.* **96**, 63–82 (1999).
6. Boyd, E. S. et al. A late methanogen origin for molybdenum-dependent nitrogenase. *Geobiology* **9**, 221–232 (2011).
7. Chen, M. Y. et al. Phylogenomics uncovers evolutionary trajectory of nitrogen fixation in cyanobacteria. *Mol. Biol. Evol.* **39**, msac171 (2022).
8. Berman-Frank, I., Lundgren, P. & Falkowski, P. Nitrogen fixation and photosynthetic oxygen evolution in cyanobacteria. *Res. Microbiol.* **154**, 157–164 (2003).
9. Fay, P. Oxygen relations of nitrogen fixation in cyanobacteria. *Microbiol. Rev.* **56**, 340–373 (1992).
10. Staal, M., Rabouille, S. & Stal, L. J. On the role of oxygen for nitrogen fixation in the marine cyanobacterium Trichodesmium sp. *Environ. Microbiol.* **9**, 727–736 (2007).
11. Allen, J. F., Thake, B. & Martin, W. F. Nitrogenase inhibition limited oxygenation of Earth's Proterozoic atmosphere. *Trends Plant Sci*. **24**, 1022–1031 (2019).
12. Butterfield, N. J. Proterozoic photosynthesis - a critical review. *Palaeontology* **58**, 953–972 (2015).

13. Hammerschmidt, K., Landan, G., Tria, F. D. K., Alcorta, J. & Dagan, T. The order of trait emergence in the evolution of cyanobacterial multicellularity. *Genome Biol. Evol.* **13**, 1–10 (2021).
14. Pang, K. et al. Nitrogen-fixing heterocystous cyanobacteria in the Tonian period. *Curr. Biol.* **28**, 616–622.e1 (2018).
15. Stal, L. J. Cyanobacterial mats and stromatolites. In: *The Ecology of Cyanobacteria* (ed, Whitton, B) pp. 61–120 (Springer Dordrecht 2012).
16. Towe, K. M. Evolution of nitrogen fixation. *Science* **295**, 798–799 (2002).
17. Scott, C. et al. Tracing the stepwise oxygenation of the Proterozoic ocean. *Nature* **452**, 456–459 (2008).
18. Zerkle, A. L., House, C. H., Cox, R. P. & Canfield, D. E. Metal limitation of cyanobacterial N2 fixation and implications for the Precambrian nitrogen cycle. *Geobiology* **4**, 285–297 (2006).
19. Boyd, E. S., Hamilton, T. L. & Peters, J. W. An alternative path for the evolution of biological nitrogen fixation. *Front. Microbiol.* **2**, 1–11 (2011).
20. Kasting, J. F. & Siefert, J. L. The nitrogen fix. *Nature* **412**, 26–27 (2001).
21. Fani, R., Gallo, R. & Liò, P. Molecular evolution of nitrogen fixation: the evolutionary history of the nifD, nifK, nifE, and nifN genes. *J. Mol. Evol.* **51**, 1–11 (2000).
22. Menor Salván, C. et al. Prebiotic Origin of Pre-RNA building blocks in a urea "Warm Little Pond" scenario. *ChemBioChem* **21**, 3504–3510 (2020).
23. Veaudor, T., Cassier-Chauvat, C. & Chauvat, F. Genomics of urea transport and catabolism in cyanobacteria: biotechnological implications. *Front. Microbiol*. **10**, 02052 (2019).
24. Mobley, H. L., Island, M. D. & Hausinger, R. P. Molecular biology of microbial ureases. *Microbiol. Rev.* **59**, 451–480 (1995).
25. Kappaun, K., Piovesan, A. R., Carlini, C. R. & Ligabue-Braun, R. Ureases: historical aspects, catalytic, and non-catalytic properties – a review. *J. Adv. Res.* **13**, 3–17 (2018).
26. Konhauser, K. O. et al. Oceanic nickel depletion and a methanogen famine before the Great Oxidation event. *Nature* **458**, 750–753 (2009).
27. Segura, A. et al. Ozone concentrations and ultraviolet fluxes on Earth-like planets around other stars. *Astrobiology* **3**, 689–708 (2003).
28. Mloszewska, A. M. et al. UV radiation limited the expansion of cyanobacteria in early marine photic environments. *Nat. Commun.* **9**, 3088 (2018).
29. Lohrmann, R. Formation of urea and guanidine by irradiation of ammonium cyanide. *J. Mol. Evol.* **1**, 263–269 (1972).
30. Malhotra, S., Pandit, M., Kapoor, J. C. & Tyagi, D. K. Photo-oxidation of cyanide in aqueous solution by the UV/H2O2 process. *J. Chem. Technol. Biotechnol.* **80**, 13–19 (2005).
31. Todd, Z. R., Wogan, N. F. & Catling, D. C. Favorable environments for the formation of ferrocyanide, a potentially critical reagent for origins of life. *ACS Earth Space Chem.* **8**, 221–229 (2024).
32. Catling, D. C. & Zahnle, K. J. The Archean atmosphere. *Sci. Adv.* **6**, eaax1420 (2020).
33. Ueno, Y., Yamada, K., Yoshida, N., Maruyama, S. & Isozaki, Y. Evidence from fluid inclusions for microbial methanogenesis in the early Archaean era. *Nature* **440**, 516–519 (2006).
34. Zahnle, K. J. Photochemistry of methane and the formation of hydrocyanic acid (HCN) in the Earth's early atmosphere. *J. Geophys Res* **91**, 2819–2834 (1986).
35. Chameides, W. L. & Walker, J. C. G. Rates of fixation by lightning of carbon and nitrogen in possible primitive atmospheres. *Orig. Life* **11**, 291–302 (1981).
36. Kasting, J. F. Bolide impacts and the oxidation state of carbon in the Earth's early atmosphere. *Orig. Life Evol. Biosphere* **20**, 199–231 (1990).
37. Todd, Z. R. & Öberg, K. I. Cometary delivery of hydrogen cyanide to the early Earth. *Astrobiology* **20**, 1109–1120 (2020).
38. Bada, J. L. & Miller, S. L. Ammonium ion concentration in the primitive ocean. *Science* **159**, 423–425 (1968).
39. Tian, F., Kasting, J. F. & Zahnle, K. Revisiting HCN formation in Earth's early atmosphere. *Earth Planet Sci. Lett.* **308**, 417–423 (2011).
40. Yang, J. et al. Ammonium availability in the Late Archaean nitrogen cycle. *Nat. Geosci.* **12**, 553–557 (2019).
41. Navarro-González, R., McKay, C. P. & Mvondo, D. N. A possible nitrogen crisis for Archaean life due to reduced nitrogen fixation by lightning. *Nature* **412**, 61–64 (2001).
42. Mather, T. A., Pyle, D. M. & Oppenheimer, C. Tropospheric volcanic aerosol. In *Geophysical Monograph Series* 139 (AGU, 2003).
43. Nishizawa, M. et al. Stable abiotic production of Ammonia from nitrate in komatiite-hosted hydrothermal systems in the Hadean and Archean oceans. *Minerals* **11**, 321 (2021).
44. Brandes, J. A., Hazen, R. M. & Yoder, H. S. Inorganic nitrogen reduction and stability under simulated hydrothermal conditions. *Astrobiology* **8**, 1113–1126 (2008).
45. Kasting, J. F. Stability of ammonia in the primitive terrestrial atmosphere. *J. Geophys. Res. Oceans* **87**, 3091–3098 (1982).
46. Panyachariwat, N. & Steckel, H. Stability of urea in solution and pharmaceutical preparations. *J. Cosmet. Sci.* **65**, 187–195 (2014).
47. Gan, D. et al. Urea-mediated warm ponds: prebiotic formation of carbamoyl amino acids on the primordial Earth. *Earth Planet Sci. Lett.* **607**, 118072 (2023).
48. Navarro-González, R., Negrón-Mendoza, A. & Chacón, E. The γ-irradiation of aqueous solutions of urea. Implications for chemical evolution. *Orig. Life Evol. Biosph.***19**, 109–118 (1989).
49. Stribling, R. & Miller, S. L. Energy yields for hydrogen cyanide and formaldehyde syntheses: The hcn and amino acid concentrations in the primitive ocean. *Orig. Life Evol. Biosph.***17**, 261–273 (1987).
50. Kieke, M. L., Schoppelrei, J. W. & Brill, T. B. Spectroscopy of hydrothermal reactions. 1. The CO2-H2O system and kinetics of urea decomposition in an FTIR spectroscopy flow reactor cell operable to 725 K and 335 bar. *Journal of Physical Chemistry* **100**, 7455–7462 (1996).
51. Elderfield, H. & Schultz, A. Mid-ocean ridge hydrothermal fluxes and the chemical composition of the ocean. *Annu. Rev. Earth Planet Sci.* **24**, 191–224 (1996).
52. Edmond, J. M. Hydrothermal activity at mid-ocean ridge axes. *Nature* **290**, 87–88 (1981).
53. Mazzei, L., Musiani, F. & Ciurli, S. The structure-based reaction mechanism of urease, a nickel dependent enzyme: tale of a long debate. *J. Biol. Inorg. Chem*. **25**, 829–845 (2020).
54. Sakamoto, T., Delgaizo, V. B. & Bryant, D. A. Growth on urea can trigger death and peroxidation of the cyanobacterium Synechococcus sp. strain PCC 7002. *Appl. Environ. Microbiol.* **64**, 2361–2366 (1998).
55. Muñoz-Velasco, I. et al. Methanogenesis on early stages of life: ancient but not primordial. *Orig. Life Evol. Biosph.* **48**, 407–420 (2018).
56. Tian, H., Fotidis, I. A., Kissas, K. & Angelidaki, I. Effect of different ammonia sources on aceticlastic and hydrogenotrophic methanogens. *Bioresour. Technol.* **250**, 390–397 (2018).
57. Sakamoto, T. & Bryant, D. A. Requirement of nickel as an essential micronutrient for the utilization of urea in the marine cyanobacterium synechococcus sp. PCC 7002. *Microbes Environ.* **16**, 177–184 (2001).
58. MacOmber, L. & Hausinger, R. P. Mechanisms of nickel toxicity in microorganisms. *Metallomics* **3**, 1153–1162 (2011).
59. Konhauser, K. O. et al. The Archean nickel famine revisited. *Astrobiology* **15**, 804–815 (2015).
60. Zaborska, W., Krajewska, B. & Olech, Z. Heavy metal ions inhibition of jack bean urease: potential for rapid contaminant probing. *J. Enzym. Inhib. Med. Chem.* **19**, 65–69 (2004).
61. Tostevin, R. & Ahmed, I. A. M. Micronutrient availability in Precambrian oceans controlled by greenalite formation. *Nat. Geosci.* **16**, 1188–1193 (2023).

62. Battistuzzi, F. U., Feijao, A. & Hedges, S. B. A genomic timescale of prokaryote evolution: insights into the origin of methanogenesis, phototrophy, and the colonization of land. *BMC Evol. Biol.* **4**, 1–14 (2004).
63. Schirrmeister, B. E., Sanchez-Baracaldo, P. & Wacey, D. Cyanobacterial evolution during the Precambrian. *Int. J. Astrobiol.* **15**, 187–204 (2016).
64. Sánchez-Baracaldo, P. & Cardona, T. On the origin of oxygenic photosynthesis and Cyanobacteria. *New Phytol.* **225**, 1440–1446 (2020).
65. Flannery, D. T. & Walter, M. R. Australian Journal of Earth Sciences Archean tufted microbial mats and the Great Oxidation Event: new insights into an ancient problem Archean tufted microbial mats and the Great Oxidation Event: new insights into an ancient problem. *Aust. J. Earth Sci.* **59**, 1–11 (2012).
66. Anbar, A. D. et al. A whiff of oxygen before the Great Oxidation event. *Science* **317**, 1900–1903 (2007).
67. Crowe, S. A. et al. Atmospheric oxygenation three billion years ago. *Nature* **501**, 535–538 (2013).
68. Planavsky, N. J. et al. Evidence for oxygenic photosynthesis half a billion years before the Great Oxidation Event. *Nat. Geosci.* **7**, 283–286 (2014).
69. Bekker, A. & Holland, H. D. Oxygen overshoot and recovery during the early Paleoproterozoic. *Earth Planet Sci. Lett.* **317–318**, 295–304 (2012).
70. Partin, C. A. et al. Large-scale fluctuations in Precambrian atmospheric and oceanic oxygen levels from the record of U in shales. *Earth Planet Sci. Lett.* **369–370**, 284–293 (2013).
71. Tyrrell, T. The relative influences of nitrogen and phosphorus on oceanic primary production. *Nature* **400**, 525–531 (1999).
72. Holland, H. D. Volcanic gases, black smokers, and the great oxidation event. *Geochim. Cosmochim. Acta* **66**, 3811–3826 (2002).
73. Reinhard, C. T. et al. Evolution of the global phosphorus cycle. *Nature* **541**, 386–389 (2017).
74. Hao, J., Knoll, A. H., Huang, F., Hazen, R. M. & Daniel, I. Cycling phosphorus on the Archean Earth: part I. Continental weathering and riverine transport of phosphorus. *Geochim. Cosmochim. Acta* **273**, 70–84 (2020).
75. Hao, J. et al. Cycling phosphorus on the Archean Earth: part II. Phosphorus limitation on primary production in Archean ecosystems. *Geochim. Cosmochim. Acta* **280**, 360–377 (2020).
76. Johnson, B. W. & Wing, B. A. Limited Archaean continental emergence reflected in an early Archaean 18O-enriched ocean. *Nat. Geosci.* **13**, 243–248 (2020).
77. Farr, O. et al. Archean phosphorus recycling facilitated by ultraviolet radiation. *Proc. Natl Acad. Sci.* **120**, e2307524120 (2023).
78. Solovchenko, A. et al. Phosphorus feast and famine in cyanobacteria: is luxury uptake of the nutrient just a consequence of acclimation to its shortage? *Cells* **9**, 1933 (2020).
79. Jentzsch, L., Grossart, H.-P., Plewe, S., Schulze-Makuch, D. & Goldhammer, T. Response of cyanobacterial mats to ambient phosphate fluctuations: phosphorus cycling, polyphosphate accumulation and stoichiometric flexibility. *ISME Commun.* **3**, 6 (2023).
80. Armstrong, C. T. et al. Impact of nitrogen chemical form on the isotope signature and toxicity of a marine dinoflagellate. *Mar. Ecol. Prog. Ser.* **602**, 63–76 (2018).
81. Waser, N. A. et al. Nitrogen isotope fractionation during nitrate, ammonium and urea uptake by marine diatoms and coccolithophores under various conditions of N availability. *Mar. Ecol. Prog. Ser.* **169**, 29–41 (1998).
82. Waser, N. A. D., Harrison, P. J., Nielsen, B., Calvert, S. E. & Turpin, D. H. Nitrogen isotope fractionation during the uptake and assimilation of nitrate, nitrite, ammonium, and urea by a marine diatom. *Limnol. Oceanogr.* **43**, 215–224 (1998).
83. Ribas, I. & Guinan, E. F. Evolution of the solar magnetic activity over time and effects on planetary atmospheres. *Symp. Int. Astronom. Union* **219**, 423–430 (2004).
84. Sebree, J. A., Stern, J. C., Mandt, K. E., Domagal-Goldman, S. D. & Trainer, M. G. 13C and 15N fractionation of CH4/N2 mixtures during photochemical aerosol formation: relevance to Titan. *Icarus* **270**, 421–428 (2016).
85. Kuga, M. et al. Nitrogen isotopic fractionation during abiotic synthesis of organic solid particles. *Earth Planet Sci. Lett.* **393**, 2–13 (2014).
86. Stevens, S. E., Patterson, C. O. P. & Myers, J. The production of hydrogen peroxide by blue-green algae: a survey. *J. Phycol*. **9**, 427–430 (1973).
87. Erratt, K. J., Creed, I. F. & Trick, C. G. Comparative effects of ammonium, nitrate and urea on growth and photosynthetic efficiency of three bloom-forming cyanobacteria. *Freshw. Biol.* **63**, 626–638 (2018).
88. Zavřel, T., Sinetova, M. A. & Červený, J. Measurement of chlorophyll a and carotenoids concentration in cyanobacteria. *Bio Protoc.* **5**, 1–5 (2015).
89. Ritchie, R. J. Consistent sets of spectrophotometric chlorophyll equations for acetone, methanol and ethanol solvents. *Photosynth Res.* **89**, 27–41 (2006).
90. Ratnayake, D. M., Tanaka, R. & Nakamura, E. Novel nickel isolation procedure for a wide range of sample matrices without using dimethylglyoxime for isotope measurements using MC-ICP-MS. *Anal. Chim. Acta* **1181**, 338934 (2021).
91. Waldbauer, J., Zimmerman, A. A. Measuring urea concentrations in water samples. *Protocols* **10**, 17504 (2022)

Acknowledgements

The authors thanks Masahiro Yamanaka, Tsutomu Ota, Christian Potiszil, and Kayo Tanaka for their technical support and anonymous reviewers for their constructive comments in improving the manuscript. Funding was provided by JSPS KAKENHI (20K04108, 23K17707 & 24K00745) and JST SPRING (JPMJSP2126) grants.

Author contributions

Conceptualization: D.M.R. and R.T. Experiment design and data acquisition: D.M.R. Funding acquisition: R.T. and D.M.R. Writing of the original draft: D.M.R. and R.T. Review and editing the manuscript: D.M.R, R.T, and E.N.

Competing interests

The authors declare no competing interests.

Additional information

Supplementary information The online version contains supplementary material available at https://doi.org/10.1038/s43247-025-02576-8.

Correspondence and requests for materials should be addressed to Dilan M. Ratnayake or Ryoji Tanaka.

Peer review information *Communications Earth & Environment* thanks the anonymous reviewers for their contribution to the peer review of this work. Primary Handling Editors: D'Arcy Meyer Dombard, Joe Aslin and Carolina Ortiz Guerrero. A peer review file is available.